

EFFECT OF NANOPARTICLE DISPERSIONS IN BINARY NITRATE SALT AS  
THERMAL ENERGY STORAGE MATERIAL IN CONCENTRATED SOLAR  
POWER APPLICATIONS

by

BHARATH DUDDA

Presented to the Faculty of the Graduate School of  
The University of Texas at Arlington in Partial Fulfillment  
of the Requirements  
for the Degree of

MASTER OF SCIENCE IN MECHANICAL ENGINEERING

THE UNIVERSITY OF TEXAS AT ARLINGTON

May 2013

Copyright © by Bharath Dudda 2013

All Rights Reserved

To my Dad (Srivatsa), my mom (Roopa), and Srihari ( my father figure) without  
whom i could not have achieved any of these.

## ACKNOWLEDGEMENTS

There are a lot of people I would like to thank who have been crucial to the success of this dissertation. First and foremost I thank my thesis supervisor, Dr.Donghyun Shin, who has helped me immensely and put up with my mistakes and silly doubts. This dissertation and all the publications would never have been possible without his support. I would also like to acknowledge the committee members Dr.Dereje Agonafer and Dr.Hyejin Moon for their patience and support. I would like to extend a special thanks to Dr. Hyejin Moon, whose course was immensely helpful in framing a lot of my results and discussions through a very educative course, namely Microscale Energy Transport. A special thanks to my friend Sriram Srinivasan who constantly helped me with my thesis and without him this dissertation would have never been completed on time. I would like to thank Rohit Sridharan for his helpful hand in proof reading of my dissertation. I thank all my dear friends Nitesh, Vishok, Shreyas, Alok and Kiran for their moral support throughout this reserach. A special thanks to Ritika for her constant encouragement, moral support and putting up with my hectic schedule. I also thank my nanomaterial research team, Hani Tiznobaik and Ramaprasath Devaradjane for their helpful contributions to my study.This disseration is dedicated to my beloved parents, my father D.C.Srivathsa and my mother Roopa, who have made me what i am today. I would like to thank them for their love and caring support. A special thanks to my brother D.S.Jayanth who always believed in me.

April 19, 2013



## ABSTRACT

# EFFECT OF NANOPARTICLE DISPERSIONS IN BINARY NITRATE SALT AS THERMAL ENERGY STORAGE MATERIAL IN CONCENTRATED SOLAR POWER APPLICATIONS

Bharath Dudda, M.S.

The University of Texas at Arlington, 2013

Supervising Professor: Donghyun Shin

Despite the huge improvements in the field of solar energy to produce electricity, the high cost of production has been one of the major problems in this field. Concentrated solar power (CSP) uses a number of mirrors to concentrate solar radiant energy onto a single focal point. Electrical power is produced when the concentrated light is converted to heat, which drives a heat engine connected to an electrical power generator. This heat is first stored in a thermal energy storage (TES) and transferred to a heat engine to be converted to electricity and thus TES can provide heat even after the sunset for extended hour of power production. Hence, the key for reducing the cost of electricity mainly relies on the operating temperature of TES, since it will determine the thermal to electric conversion efficiency. Increasing TES operating temperature can enhance the cycle efficiency and as a result the cost of electricity can be reduced. However, traditional TESs such as paraffin wax and fatty acid are likely to decompose at high temperatures (300 400 C). Molten salts can achieve higher temperatures leading to higher efficiency and lower costs. Hence,

they have caught the attention of researchers as a potential substitute for traditional TESs. Molten salts can achieve higher temperatures leading to higher efficiency and lower cost. However, poor thermo-physical properties of molten salts were one of the most challenging problems. It has been recently found that doping of nanoparticles in molten salts significantly enhance their thermo-physical properties. In this study, eutectic of sodium nitrate and potassium nitrate at 60:40 by weight were chosen as the base molten salt and silica nanoparticles were used to enhance the specific heat capacity of the salts. A modulated differential scanning calorimeter (MDSC) was employed to measure the specific heat capacity of the TESs. Different sizes (5, 10, 30 and 60 nanometers) of nanoparticles were considered to investigate if the size of the nanoparticle had an effect on the specific heat capacity. It was seen that the doping of nanoparticles enhanced the specific heat capacity by approximately 27% for 60nm. Material characterization was carried out using the Scanning Electron Microscope (SEM) to explore the cause of the enhanced specific heat capacity and it was found that the nano-engineered molten salts were filled with distinct nanostructures. It was observed that as the amount of nanostructures increased the enhancement of specific heat capacity also increased. This finding would lead to decrease in amount of TES used in the power plants which leads to a decrease in the size of the thermal storage tank and eventually reduces this total cost.

## TABLE OF CONTENTS

ACKNOWLEDGEMENTS . . . . .	iv
ABSTRACT . . . . .	v
LIST OF ILLUSTRATIONS . . . . .	ix
LIST OF TABLES . . . . .	xii
Chapter	Page
1. INTRODUCTION . . . . .	1
1.1 introduction . . . . .	1
1.2 Concentrated solar power: . . . . .	2
1.2.1 History . . . . .	2
1.3 What is concentrated solar power? . . . . .	2
1.4 CSP and its componenets . . . . .	3
1.4.1 Parabolic troughs . . . . .	3
1.4.2 Concentrating Dish/ Striling Engines . . . . .	4
1.4.3 Power tower system . . . . .	5
1.5 Thermal energy storage . . . . .	6
1.5.1 Thermocline . . . . .	7
1.5.2 Two tank storage . . . . .	9
1.6 Challenges of CSP . . . . .	10
1.7 Solar salt: Molten nitrate salt eutectic as TES material . . . . .	11
1.8 significance of this study . . . . .	13
1.9 Nanofluids . . . . .	14
1.10 Ionic-based Nanofluids . . . . .	14

1.11 Objective of this study . . . . .	15
1.12 motivation of the study . . . . .	16
2. EXPERIMENTAL SETUP . . . . .	17
2.1 Information on the salt eutetic and nanoparticles used . . . . .	17
2.2 Nanofabrication of molten salt with nanoparticles . . . . .	18
2.3 Sample preparation for testing in MDSC . . . . .	19
2.4 Modulated differential scanning calorimeter (MDSC) . . . . .	20
2.5 Testing procedure using MDSC . . . . .	21
3. RESULTS AND DISCUSSIONS . . . . .	22
3.1 Specific heat results from MDSC . . . . .	22
3.2 Material characterization . . . . .	28
3.3 Nanostructures . . . . .	36
4. CONCLUSION . . . . .	39
Appendix	
REFERENCES . . . . .	41
BIOGRAPHICAL STATEMENT . . . . .	47

## LIST OF ILLUSTRATIONS

Figure	Page
1.1 Block Diagram of CSP[1] . . . . .	3
1.2 Parabolic Trough . . . . .	4
1.3 Concentrating Dish . . . . .	5
1.4 Power Tower System . . . . .	6
1.5 Block Diagram of a Thermocline[42] . . . . .	9
1.6 Block Diagram of Two Tank[42] . . . . .	11
3.1 The variation of specific heat capacity with temperature for the pure eutectic and the nanomaterials (5 nm, 10 nm, 30 nm and 60 nm) in the full temperature range (150 C – 450 C). . . . .	25
3.2 The variation of specific heat capacity with temperature for the pure eutectic and the nanomaterials (5 nm, 10 nm, 30 nm and 60 nm) in the solid phase (150 C – 190 C). The specific heat capacity of nanomaterials samples were enhanced by 3-10 % in comparison with the pure eutectic and slightly increased with nanoparticle size. . . . .	26
3.3 The variation of specific heat capacity with temperature for the pure eutectic and the nanomaterials (5 nm, 10 nm, 30 nm and 60 nm) in the liquid phase (250 C – 450 C). The specific heat capacity of nanomaterials samples were enhanced by 10-28 % in comparison with the pure eutectic and increased with nanoparticle size. . . . .	27
3.4 The variation of specific heat capacity with different nanoparticle sizes (liquid phase). . . . .	28

3.5	The pure nitrate eutectic structure without nanoparticles. This is a back scattered electron image and no significant difference in contrast was observed. . . . .	31
3.6	5 nm nanomaterial structure. Comparing with pure eutectic structure (Fig. 3.5), a few small structural changes are rarely observed. (bright area in the image) A high resolution image of these changes is available in Fig. 3.10. This sample shows less than 10 % enhanced specific heat capacity compared with that of pure salt eutectic. . . . .	32
3.7	10 nm nanomaterial structure. The contrast difference shown in the backscattered electron image clearly shows the nanostructures formed by the salt eutectic. Comparing with 5 nm nanomaterial (Fig. 3.6), the observed amount of nanostructures is increased. This sample shows 13 % enhanced specific heat capacity compared with that of pure salt eutectic. . . . .	33
3.8	30 nm nanomaterial structure. The contrast difference shown in the backscattered electron image clearly shows the nanostructures formed by the salt eutectic. The quantitative increase of nanostructures is clearly visible here. The amount of nanostructures clearly increased compared with 5 nm (Fig. 3.6) and 10 nm (Fig. 3.7) samples. This sample shows 21 % enhanced specific heat capacity compared with that of pure salt eutectic. . . . .	34
3.9	60 nm nanomaterial structure. This sample shows the highest enhancement in specific heat capacity (28 %) compared with that of pure salt eutectic. It is shown in the figure that nanostructures are present almost everywhere. The presence of the large amount of nanostructures can be responsible for the high enhancement in specific heat capacity. . . . .	35

3.10	A high resolution image of the small structural change found in 5 nm nanomaterial (Fig. 3.6). In this portion of nanomaterial, salt eutectic molecules seem to form very small structures resembling particles, threads, or webs at the size of 10-100 nm (nanostructure). . . . .	36
------	--	----

## LIST OF TABLES

Table		Page
3.1	Specific heat capacity of base eutectic and nanomaterials (solid phase)	24
3.2	Specific heat capacity of base eutectic and nanomaterials (liquid phase)	24



# CHAPTER 1

## INTRODUCTION

### 1.1 introduction

Non renewable sources serve most of the production needs of electricity. In order to ensure that we preserve fossil fuels, there is an urgent need for an alternative source of electricity. Although our access to the vast reserves of clean renewable energy such as solar, tidal, wind or geothermal energies can meet our energy demands, solar energy has emerged as the feasible solution to this energy crisis. The sun provides us with 120,000 Tera watts of energy per hour.[2] It has been estimated that the amount of sunshine in these types of areas when exploited in an efficient way would extract around 120 GWh of electricity per year from a surface area of 1 km<sup>2</sup>. This amount of energy obtained through the means of solar power is equivalent to an annual production of a traditional 50 MW power station powered by coal or natural gas.[3] Speaking of the solar energy as a source to generate electricity, the two major factors that have the maximum impact is the cost and the storage of the energy. Since, sunlight is available for just limited amount of time in a day it was a major challenge to produce the electricity in the later stages of the day. Lately, the technology of concentrated solar power (CSP) has been emerging as the feasible potential to utilize the solar power, store the sun's energy and make use of the stored heat to generate electricity in the later stages of the day. The potential to store energy cost-effectively and to deliver this as electricity when needed is a huge task and also the greatest strength of the CSP compared to other forms of energy harvesting. Generally the storage of energy leads to the need of expensive batteries or conversion of these

stored energies into other forms which are often very inefficient and expensive. In this regard, CSP has a huge upper hand as it can store the suns energy when it is at the peak and deliver that power when there is need i.e. in the later stages of the day. [4]

## 1.2 Concentrated solar power:

### 1.2.1 History

Since the 1980's many countries like Spain, United states and Germany have been looking up to concentrated solar power as a potential substitute to the non-renewable sources for power generation. In the 1970's period of energy crisis, a lot of them invested funds for a spectrum of renewable energy sources.[5] During which nine solar plants were constructed in the southwestern U.S from the period of 1980's-1990's. These plants which are still in operation were ranging in size from 14 to 80 MW with a capacity of 354 MW.[5] But these plants produced the power reliably for decades they had a major setback on the expenses side. Due to the low prices of fossil fuels at that period the CSP was dried up. But the concerns about the energy security and issues of global warming attracted these countries towards new innovations that have reduced costs, improved efficiency of CSP systems and brought back the focus on the CSP yet again to tackle the energy crisis. [5]

### 1.3 What is concentrated solar power?

Concentrated solar power uses systems use mirrors or lenses to concentrate a large area of sunlight onto a small area. Electrical power is produced when the concentrated light is converted to heat, which drives a heat engine (usually a steam turbine) connected to an electrical power generator. [6] CSP gives the option of

thermal storage which enables the plant to produce power under cloud cover and at later stages of the day when the demand for the electricity is maximum.

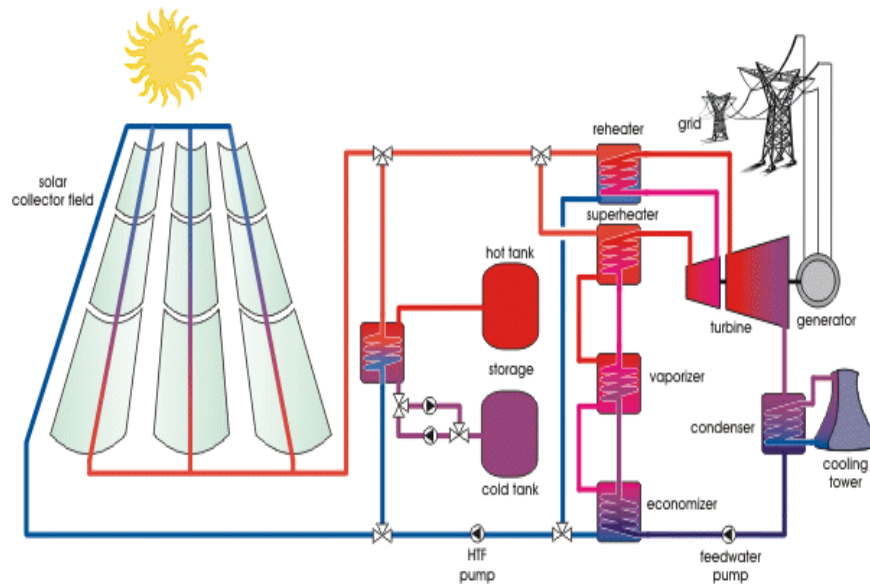


Figure 1.1. Block Diagram of CSP[1].

#### 1.4 CSP and its componenets

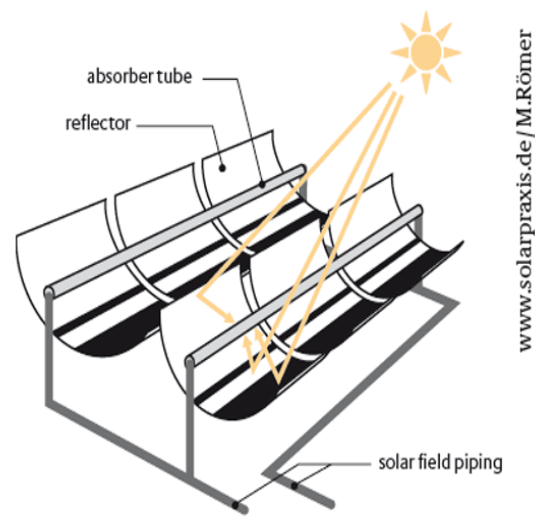
As discussed above the CSP tried to concentrate the sunlight onto a small area. To concentrate the sunlight it uses various technologies namely parabolic troughs, concentrating dishes, the central receivers each of which are explained below in detail.

##### 1.4.1 Parabolic troughs

Parabolic troughs are the most popular form of CSP for delivering utility-scale power. The parabolic troughs have mirrors shaped in parabolic form. The whole point of focus of the suns rays are reflected towards the center where an absorption tube is suspended. There are superheated fluids which are heated and keeps traveling



(a) Picture of a Parabolic Trough[7]



(b) Block Diagram of a Parabolic Trough[8]

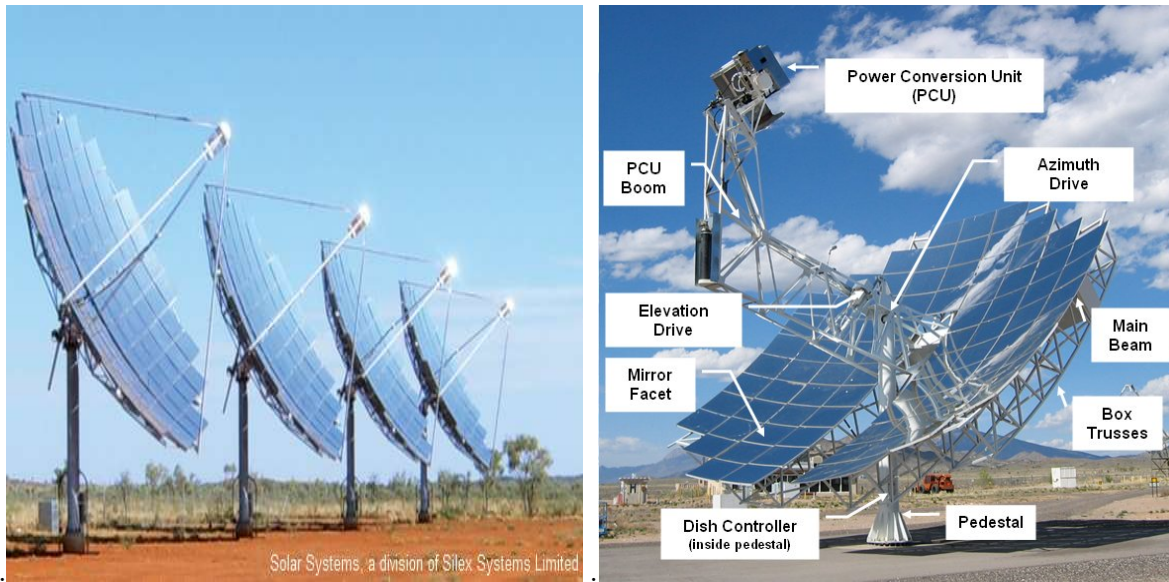
Figure 1.2. Parabolic Trough.

through this special tubes towards the collecting unit. There it gets heated and generates steam to power turbines. [5] Recent technological advances have been huge in the field of parabolic troughs. Latest power plants such as the Nevada Solar One, 164MW facility that went on line in July 2007, have shown huge improvements in the technology related to increase in efficiency. There are a number of research going on to eliminate ball-joints and increase systems thermal capacity. Molten salt has also become a point of focus as the High technology HTFs and storage materials to reduce cost by directly producing steam inside the special absorption tubes. [5] In addition, proposals are moving forward for new parabolic trough plants, including a 550 MW plant in California and a 280 MW facility in Arizona.[5]

#### 1.4.2 Concentrating Dish/ Stirling Engines

Concentrated dish is shaped similar to a satellite dish. It works on a similar principle to the parabolic troughs: curved mirrors reflect the sunlight on to a collecting

location at the centre of the dish. Instead of the long absorption tube, the sunlight is focused on to the central collecting location suspended above the bowl of mirrors. Because of its ability to attain very high-temperature of around 750 Celsius it heats a thermal fluid which in turn powers a small steam or Stirling engine. These dishes were most effectively used in remote areas where there is not sufficient space to install a large number of mirrors since this individual dish is a self-sufficient unit. [9]



(a) Picture of a Concentrating Dish[10]

(b) Block Diagram of a Concentrating Dish[11]

Figure 1.3. Concentrating Dish.

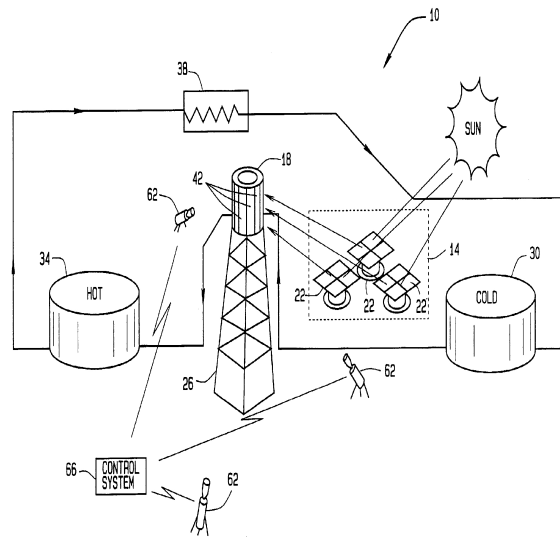
### 1.4.3 Power tower system

Central receivers (or power towers) also use mirrors to focus sunlight to a focal spot in this case, a tower. But instead of using a dish to harvest solar power, central receivers rely on a stationary tower and nearly flat, tracking mirrors (heliostats) arrayed around the tower. Each heliostat in the array is free-standing, and is able to

independently track the sun. Inside the receiving tower, a heat transfer fluid (usually water or molten salt) absorbs the sun's thermal energy and is used to generate steam for a turbine. [12] Because so much sunlight is concentrated in a small area, the tower fluid becomes superheated, reaching 650 Celsius. These higher temperatures help to reduce the cost of thermal storage. Also, the heliostats used in central receivers are nearly flat, rather than curved, reducing their manufacturing cost. These features combine to give central receivers the potential to be produced inexpensively.[12]



(a) Picture of a Power Tower[13]



(b) Block Diagram of a Power Tower[14]

Figure 1.4. Power Tower System.

### 1.5 Thermal energy storage

The heat collected through any of the above technologies (parabolic, concentrating dish or power tower) is transferred to the generating unit or storage unit by the help of heat transfer fluid (HTF). The most commonly used HTF are the mineral

oils. Lately the molten salt has caught the attention of the researchers as a potential HTF to achieve higher temperatures.[15] This HTF carries the heat to inside a boiler or to a storage area which is known as the thermal-energy storage (TES). [16] The TES are usually a large thermos tank which stores the heat collected from the sun and deliver it at the later stages of the day when the demand is maximum. The TES systems have the greatest benefit of being applicable in most power generating plants as it aids as a direct supplement to the existing electricity conversion systems, which are usually rankine cycle turbines. Thus TES prevail to be the cost-effective as it integrates with any power generating plant removing the extra charges for storage. [16, 17] TES system goes very well with the CSP power plants since both deal with the thermal energy. Its storage of heat can help produce electricity upto 7.5 hours without sunlight. Sometimes the HTF like the molten salts itself can be used as TES material to save on the cost. This is because there is always a need of additional heat exchangers in transferring the energy from the HTF to the storage material, from storage to the steam generating section. These additional heat exchangers are expected to cause a loss in efficiency upto 7%. Moreover, the trough facility which can achieve high temperatures upto  $700^{\circ}F$  (using the high temperature fluid) requires upto 3 times the amount of storage material to generate the same amount of electricity as an integrated thermal energy storage system attaining  $1050^{\circ}F$ . These factors are expected to be huge reduction in costs. There are several research carried out on this topic. [17] The different types of TES storage examples that are commonly used are explained below.

### 1.5.1 Thermocline

The Thermocline is basically a link between the collecting unit and the generating unit. But it is also possible that the HTF can be transferred from the collecting



unit to the generating unit by passing the thermocline entirely. The major parts that makes up the thermocline is the storage tank, fillers, heat exchangers and storage fluid. The huge tank is filled with fillers and the storage material. There are two heat exchangers at the two ends of the tank connecting collecting unit and generating unit. When the hot HTF is pumped through the tank containing the fillers and the storage unit. It heats up the storage unit which eventually charges the thermocline. The storage material then heats the filler by conduction and internal convection. The electricity generation system working fluid is run through the second heat exchanger linking the storage material to the electricity generation system to discharge the thermocline. The storage material chosen for this investigation is a nitrate eutectic called Hitec solar salt, which will be discussed in greater detail later. The filler is generally comprised of macro-sized solid material particles. The most common filler is processed sand. The combination of the storage material and the filler creates an aggregate thermal mass able to absorb considerable quantities of thermal energy per volume. [18] The thermocline basically has a huge advantage as it is very rigid and robust in design. Because of its huge size it can hold more energy per unit volume. The size of the thermocline can be altered as per its requirement. But on the downside, given its huge size and material it is relatively expensive. Generally the HTF and the storage material may or may not be the same. But it is preferred that they are not the same since the specific heat of the storage material needs to be higher than the HTF. The thermal conductivity plays a significant role as it determines the heat exchanger size needed to meet the power transfer capabilities of the TES system. The filler needs to have a high specific heat and be extremely cheap. The filler is used to cut the cost of the thermocline, as the filler is generally at least an order of magnitude cheaper than the storage material on a per-mass basis, while having a similar specific heat. The standard filler currently in use is sand, due to its extremely



low cost and generally inert behavior. [18] A concern in a thermocline system is the requirement that the storage material must be in a liquid form to allow for circulation in the thermocline. Keeping the storage material in liquid form can be problematic, as the most common storage materials have melting temperatures of above  $180\text{ }^{\circ}\text{C}$ . Therefore, many of the thermocline systems have auxiliary heaters to maintain the storage material in its liquid state. These heaters are frequently natural gas or electric units, so they require substantial external energy to function, increasing the cost of thermocline operation. [18]

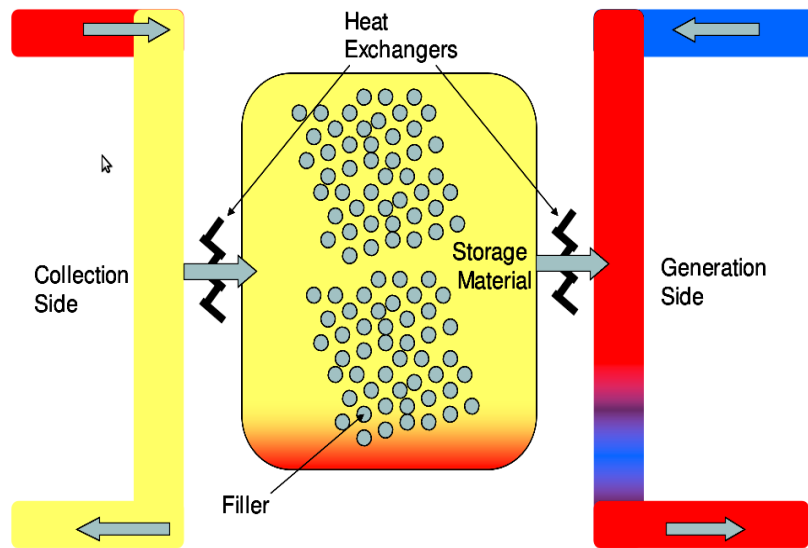


Figure 1.5. Block Diagram of a Thermocline[42].

### 1.5.2 Two tank storage

The two tank storage system is very similar to the thermoclines. Here there are two tanks present one of them cold and the other being hot. The heat exchangers are installed similarly to the thermoclines at the ends of each tanks. In this two

tank storage the connection between the tanks has the heat exchangers linked to the electricity generating cycle and also the storage material with the HTF. The two-tank storage system gets charged when the cold storage material is pumped between the two tanks so it interfaces with the HTF heat exchanger, raising the storage materials temperature. Once the storage material is through the HTF heat exchanger, it gets pumped to the hot tank. This pumping process continues till the complete storage material is been pumped through the HTF heat exchanger into the hot tank. Now the system is fully charged and is operating at its maximum temperature. The discharging process here is carried out by pumping the hot storage fluid back to the cold tank through the generation cycle heat exchanger. Here the hot storage material transfers its thermal energy to the electricity generation cycle thereby decreasing the temperature. [16, 19] The two-tank system has a huge downside when compared to thermoclines as they are relatively more expensive than the thermocline. They are much more complicated as they require pump, heat exchangers and large quantities of the storage material. Since the fillers are more cheaper than the storage material the thermoclines are more preferred by many compared to two tank storage. Fillers cannot be used in the two tank storage as they might not help enough to the pumping power and also do not well with the design of the two tank storage. [16, 19]

## 1.6 Challenges of CSP

The storage materials used in the TES was discussed in the above section. The major challenge of the CSP which is the cost factor is reliant on the TES since the size of the thermal-energy storage tank, the quantity of storage material and the Heat-transfer fluid makes up the major part of the costs. [20] Hence, several efforts were put in to finding a suitable storage materials for TES which are both inexpensive

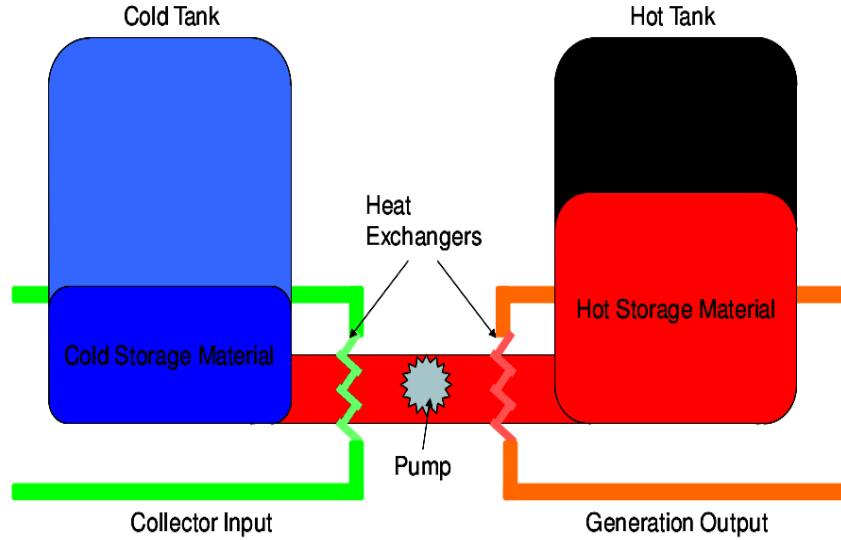


Figure 1.6. Block Diagram of Two Tank[42].

and also high on thermo-physical properties. Lately, Molten salt have caught the attention of researchers as a potential candidate for the storage material in TES. Since the molten salt can be heated upto higher temperatures and thus higher-efficiency are achievable. [21] Since they are stable upto temperatures of 1000 degree Celsius ,it allows the solar field to heat the HTF to a higher temperature. Higher temperature operation of the solar field reduces the cost of thermal storage because the volume of storage material and the size of the storage vessels are reduced. [22] The usage of molten salt HTF eliminates the need of separate fluids in solar field and storage system and thus eliminates the need of heat exchangers between the solar field and thermal-energy storage system.[22]

### 1.7 Solar salt: Molten nitrate salt eutectic as TES material

There are several solar thermal power plants in construction now. Most of them are now employing the molten salt as their HTF. Most of the promising solutions for

the storage materials are also done by molten salt. The currently used storage material is the nitrate salt eutectic which consists of mixture of sodium nitrate ( $\text{NaNO}_3$ ) 60% - potassium nitrate ( $\text{KNO}_3$ ) 40% by weight.[23] This same mixture is also used as the heat transfer fluid (HTF). This nitrate salt eutectic is used in most of the power plants like the Andasol 1, 2 and 3 [24].The nitrate salt eutectic is very stable at high temperatures upto  $1050\text{ }^\circ\text{F}$  which allows high energy steam to be generated at standard temperatures which in turn increaes thermodynamic efficiencies. [25] This nitrate salt eutectic is considered the best possible option because of its lower operating pressure and better heat transfer and thus higher allowable incident flux than a water/steam receiver. This translates into a smaller, more efficient, and lower cost receiver and support tower. In addition, the relatively inexpensive salt can be stored in large tanks at atmospheric pressure, allowing 1) economic and efficient storage of thermal power collected early in the day for use during peak demand periods; 2) increased plant capacity factor by oversizing of the collector and receiver systems with storage of the excess thermal energy for electricity generation in the evening; 3) isolation of the turbine-generator from solar energy transients; and 4) operation of the turbine at maximum efficiency. [26, 27] If necessary, a molten salt system can be hybridized with fossil fuel in a number of possible configurations to meet demand requirements when the sun is not shining. Several research are being carried out to translate the HTF with better thermal properties and lower melting points. But currently the mixture of sodium nitrate (60%) and potassium nitrate (40%) by weight is the best option.[27] The most important thing to be noticed about the nitrate eutectic here is specific heat, which is the primary objective of this research, the latent heat of fusion and the melting point. Although the molten salt has many advantages it has its own set of disadvantages. The solar thermal power are heavily dependant on the high temperature thermal storage units for continious

operation. Typical storage units such as mineral oil based storage are stable only till  $400\text{ }^{\circ}\text{C}$  . It would be a huge potential if this temperature range is pushed to higher limits such as  $500\text{-}600\text{ }^{\circ}\text{C}$ . Although the molten salt can reach higher temperatures than this the thermo-physical properties is very low. Especially the specific heat capacity is very poor.[28] It is  $2\text{ kJ/kg}^{\circ}\text{C}$  and hence may lead to dramatic increase in size of HTF / TES. [23] If this thermophysical property can be enhanced the solar thermal power could become more competitive with coal fired power plants in near future. [29]

### 1.8 significance of this study

This study revolves around the field of enhancing the specific heat capacity which is an important thermo-physical property of the molten salt eutectic. In order to contribute to the cost reduction strategies of CSP, this study presents a potential HTF/TES candidate as the molten nitrate nanomaterials. Recently the nanofluids are becoming hugely popular in enhancing the thermo-physical properties hence the methods of fabricating the molten salt with nanoparticles are also presented in detail. The enhancement of specific heat capacity without compromising on the other thermo-physical properties like thermal conductivity and viscosity was the primary focus of this study. National laboratories like the Argonne National Laboratories, Savannah National Laboratories are now focusing on this field of enhancing the specific heat capacity of the molten salt doping of nanoparticles. An increase of volumetric heat capacity translates into a better heat transfer fluid as more energy is stored per volumetric unit in the solar concentrating section, thus more efficiency in increased steam pressure. [30] Thus this study will be focused on addition of silica nanoparticles to the molten nitrate salt to enhance the specific heat capacity. This enhancement will surely cause an impact as this is the currently used storage material and could be

easily implemented to effectively reduce the total costs and thus the cost of production too.

## 1.9 Nanofluids

Colloidal suspension of nanometer-sized particles dispersed in a solvent material is termed as a Nanofluid.[31] These nanofluids were reported to have an anomalous enhancement of thermal conductivity when compared with the neat solvent. Water based nanofluids were proven to have enhanced thermal conductivity by 30% and 60%,when doped with aluminium oxide and copper oxide nanoparticles. [31, 32] Also oil based nanofluids were tried with carbon nanotubes and an amazing 161% enhancement in thermal conductivity was observed. [33] Thermal conductivity of ethylene glycol (EG) was enhanced by 40 % when mixed with Cu nanoparticles at 0.3% by volume.[34] The thermal conductivity of EG was enhanced by 20% when mixed with CuO nanoparticles at 4% concentration by volume.[35] The thermal conductivity of oil (poly-alpha-olefin/ PAO) was enhanced by 150% when mixed with Carbon Nanotubes (CNT) at 1 % by volume.[36] Thus the enhancement of thermal conductivity were observed with all possible nanofluids. There have been many attempts to understand these anomalous enhancements and researchers have come up with many theories. They includes: Brownian motion of nanoparticles, molecular level layering of the liquid at the liquid/particle interface, nature of heat transport in nanoparticles and nanoparticle clustering. [37, 38].

## 1.10 Ionic-based Nanofluids

Even though the water-based or oil-based nanofluids showed huge enhancements in thermal conductivity, they were not able to enhance the other important

thermo-physical property of specific heat capacity. There were contradictory reports of specific heat being decreased by 40-50% when Al<sub>2</sub>O<sub>3</sub> were doped in Al<sub>2</sub>O<sub>3</sub> water based nanofluid at 21.7% concentration.[40]. Similar to the thermal conductivity the other important thermo-physical property, the specific heat was also enhanced by doping of nanoparticles. Nelson et al [39] reported an enhancement of 50% by doping in exfoliated graphite nanoparticles at 0.6% by weight in pure polyalphaolefin. But studies on ionic based nanofluids suggest that the specific heat capacity was also enhanced without compromising on the thermo-physical properties. Shin and Banerjee [41] showed an enhancement of 14.5% in specific heat capacity of the alkali chloride salts by doping in silica nanoparticles. Nicolas et al.[30] from the Savannah National Laboratories also showed an enhancement of 30% in heat capacity by doping in Al<sub>2</sub>O<sub>3</sub> nanoparticles in ionic liquids. Betts [42] found 20% enhanced specific heat capacity of binary nitrate salt by doping in silica nanoparticles.

### 1.11 Objective of this study

The primary objective of this study is to investigate if the doping of silica nanoparticles in molten nitrate salt consisting of eutectic of Sodium-potassium nitrate at (60-40%) by weight would enhance the specific heat capacity. Since the effect of nanoparticle dispersions were to be studied different sizes of nanoparticle were used namely 5nm, 10nm,30nm and 60nm .MDSC was employed to measure the specific heat capacity of the doped nanomaterials. The obtained results were compared with the effective specific heat capacity model as shown below. Material characterization was carried out to study the structural changes that is happening when nanoparticles are doped.

$$C_{p,n} = \frac{(V_p * \rho_p * C_{p,p}) + (V_f * \rho_f * C_{p,f})}{V_p * \rho_p + V_f * \rho_f} \quad (1.1)$$

where  $C_{p,n}$  = specific heat capacity of nanomaterial  $C_{p,p}$  = specific heat capacity of nanoparticle  $C_{p,f}$  = specific heat capacity of base material  $\rho_p$  = density of nanoparticle  $\rho_f$  = density of base material  $V_p$  = volume fraction of nanoparticle  $V_f$  = volume fraction of base material

### 1.12 motivation of the study

The issue of rising prices in cost of production through CSP was focused in this study. Since the HTF/TES contributed to majority of the costs in CSP, researchers attention was concentrated on choosing a potential candidate as HTF/TES material in CSP. Reports suggested the promise behind the molten salts as potential substitutes for HTF/TES materials. It was found from earlier studies that the improvement in the thermo-physical properties especially specific heat capacity would help the storage material to store more heat energy per unit volume and thus reduce the amount of TES material used. This reduction in material leads to reduction in size of thermal storage tank and thus eventually the total costs. The huge promise of enhanced specific heat capacity in ionic based nanofluids for the reduction in cost of production for generating power and also the unknown reasons behind the anomalous enhancement motivated the urge to research on this field.



## CHAPTER 2

### EXPERIMENTAL SETUP

#### 2.1 Information on the salt eutetic and nanoparticles used

The preparation of nano-engineered molten salts are to be meticulously carried out to prevent agglomeration. The mixture prepared must be a homogeneous mixture. The Sodium-potassium nitrate powders used to prepare the nanofluids are obtained from Spectrum chemicals. The silica nanoparticles are obtained from Meliorum Technologies. Four different sizes of nanoparticles were used namely 5nm, 10nm, 30nm and 60nm. A Modulated Differential Scanning Calorimeter (MDSC) was employed to measure the specific heat capacity. The material characterization was carried out using the Scanning Electron Microscope (SEM; ZEISS Supra 55 VP) to study the phase or the structure of the material. The pure material was first studied with immense efforts to get familiar with the structure of the pure nitrate eutectic. The images of the structure of a pure eutectic were captured clearly with a secondary lens in the SEM. When an eutectic of two or more salts are mixed and the material characterization is to be carried out, it is mandatory to be able to distinguish between the two or more materials mixed in the eutectic. Hence, the Backscattered (BSD) imaging lens were used to distinguish the different material used in the salt mixture. The backscattered lens helps to distinguish the difference in materials used by displaying different contrast for different material used. Thus, the use of Backscattered lens also vindicates the question of contamination in the sample. The images of the structure of pure nitrate eutectic was captured using the BSD lens also. The images

taken using the BSD lens and secondary lens for the pure eutectic are shown in the figures.

## 2.2 Nanofabrication of molten salt with nanoparticles

In order to mix nitrate eutectic with the silica nanoparticles, a meticulous approach was carried out to get a homogeneous mixture. The method followed to fabricate the base material has three steps. The first being the mixing, second being the sonication and the final one is the dehydration. The mixing is basically addition of sodium nitrate salt of 60% by weight and potassium nitrate salt of 40% by weight composition. The silica nanoparticles at 1% by weight was added manually into the sample. The salts to be mixed were ready made salts as discussed earlier obtained from Spectrum Chemicals. The Nanoparticles were obtained from the Meliorum technologies. The use of nanoparticles created several significant challenges in the area of sample preparation. The largest challenge stems from the small size of the nanoparticles: cross- contamination. In order to prevent cross-contamination, all samples were prepared in a cleaned glovebox, and each salt type including the nanoparticles had its own tool set, meaning there was a steel pan and scraper used only for silica nanoparticles and another set used exclusively for sodium and potassium nitrates respectively. Thus, a total of 198mg of molten salt with 2mg of silica nanoparticles were mixed in a sample to be tested. The weights were tested using a microbalance (Sartorius CPA225D). This sample was stored in an empty bottle and extreme care was taken to maintain a clean environment to avoid contamination. Once the salts were mixed with nanoparticles there was a need of solvent to mix it efficiently. The solvent used to mix was distilled water. Around 20ml of distilled water was poured into the empty bottle and mixed cleanly. The process of nanofabrication always needs to be examined and carried out efficiently to avoid agglomeration since the particles

at nano size have the tendency to attract towards each other. Hence the second step of sonication was carried out. An ultrasonicator (Branson 3510, Branson Ultrasonics Co.) was employed to sonicate the mixture in order to ensure excellent dispersion of nanoparticles inside the mixture and also to avoid to the potential agglomeration of nanoparticles. To avoid this effect, the ultra-sonication process was carried out . The sample is sonicated in the ultrasonicator for approximately 200 minutes. Once the sonication was completed, the mixture was removed and the salt solution is dehydrated by placing it on a hot plate at 200 C for 7hrs. The obtained dehydrated salt was used as the testing material for the MDSC.

### 2.3 Sample preparation for testing in MDSC

Modulated differential scanning calorimeter (MDSC; Q20, TA Instruments, Inc.) was used to measure the specific heat capacity of the testing material. A total of 200mg of nitrate eutectic with nanoparticles were prepared each time before testing it in MDSC. A Tzero hermetic pan/lid (TA instruments) was used to place the samples in the MDSC. The empty pan was first measured using the same microbalance. The salt prepared was loaded into the empty pan carefully. In order to ensure the sample being loaded is free of moisture each testing material was heated to approximately 30 minutes before being loaded into the pan. The moisture absorbed material not only gives you a bad result but also damages the working of the machine. Hence extreme care was taken to avoid the moisture in the samples. The sample mass ranged from 15 - 25 mg. The Tzero hermetic pan/lid was hermetically sealed to avoid any further absorb-able moisture. The absence of moisture were confirmed by the steady heat flow signal in the MDSC.

## 2.4 Modulated differential scanning calorimeter (MDSC)

MDSC basically works on the principle of comparing the thermal energy of two samples simultaneously. One sample being the reference which is empty and the other is the loaded sample. The heat flow which is recorded is the reference thermal energy input minus the sample thermal energy input to create a single value which represents the difference in energy required to raise the temperature of the sample and reference items by the same quantity. There are two methods to get the specific heat from this information: ASTM 1269E and MDSC. [34] In this research the MDSC method were used to measure the specific heat capacity. The MDSC was considered given its precision in measuring the specific heat capacity better than the traditional DSC method. The traditional DSC method's accuracy is often less than desired (10%). This method superimposes a sinusoidal temperature variation over a fixed temperature increase rate. Using the sinusoidal temperature response of the sample and reference pans, the specific heat of the sample can be found. [34] Modulated DSC enjoys a significant advantage over standard DSC because it does not require a stable baseline to achieve high accuracy. The measurement of Reversing heat capacity is only based on the amplitude of the modulated heat flow signal and not its average value. Standard DSC uses the average heat flow rate, which is only as stable as the baseline of the instrument. That is why three runs are usually required with standard DSC and also why they must be done in immediate succession in order to obtain the best results. The Total heat capacity signal of MDSC is also based on the absolute value of the heat flow signal, but is less accurate than in standard DSC because of the slower average heating rate used.[34]

## 2.5 Testing procedure using MDSC

A standard automated procedure was implemented to perform the heat capacity measurements using the MDSC. The sample was initially maintained at 140 C to stabilize the signal of the calorimeter. The temperature was then increased linearly by 2 C/min till 500 C. The sample is then maintained at the same temperature for 5 min to check its stability and ensure steady state conditions. Same procedure was implemented repeatedly on a same sample for 3 times to ensure the repeatability of the instrument and results were recorded.

## CHAPTER 3

### RESULTS AND DISCUSSIONS

#### 3.1 Specific heat results from MDSC

The eutectic of NaNO<sub>3</sub>-KNO<sub>3</sub> at 60-40% by weight was doped with the silica nanoparticle of sizes 5nm, 10nm, 30nm and 60nm. There were 5 different samples prepared for each sizes and also the pure sample to compare the results. Each sample was tested thrice to get the repeatability. The specific heat capacity was measured by the MDSC and the graphs showing the heat flow is shown. It was observed that the melting point of the Nitrate eutectic was around 222 °C which matches well with the literature values.[42] There was no change in the melting point of nitrate eutectic when the nanoparticles were doped in. It was observed from the graph that the molten salt remains in the liquid phase for most part of the testing. The specific heat capacity of both the solid phase and liquid phase was recorded. The average specific heat capacity of the pure sample at the solid phase was observed to be 1.21  $J/g^{\circ}C$ . The average specific heat capacity of the nanomaterial at the solid phase for the 5nm, 10nm, 30nm and 60nm was found to be 1.25  $J/g^{\circ}C$ , 1.26  $J/g^{\circ}C$ , 1.27  $J/g^{\circ}C$ , and 1.34  $J/g^{\circ}C$ , respectively. The average specific heat capacity of the pure sample at liquid phase was found to be 1.47  $J/g^{\circ}C$ . The average specific heat capacity of the nanomaterial of 5nm, 10nm, 30nm and 60nm at liquid phase was found to be 1.60  $J/g^{\circ}C$ , 1.63  $J/g^{\circ}C$ , 1.73  $J/g^{\circ}C$ , and 1.81  $J/g^{\circ}C$  respectively. This shows a very high enhancement compared to the solid phase. The enhancement of the 60 nm is the highest among the samples which is approximately 27 % as shown in table 3.2. These results were compared with the conventional effective specific heat capacity

model (equation 1.1). This model based on simple mixing theory failed to predict the enhancement in both the solid and liquid phase. Since the specific heat capacity of nanoparticle and pure eutectic are about  $1.0 J/g^{\circ}C$  and  $1.6 J/g^{\circ}C$ , respectively. The nanoparticle concentration was very small (1 % by weight). Thus, estimate by the model was slightly lower than the pure eutectic.

It was observed that the 60nm nanomaterial had the highest percentage of enhancement upto 28% compared to the pure eutectic. The average enhancement of the 5nm nanomaterial was found to be 8%. The specific heat capacity of 10 nm nanomaterial was enhanced by an average of 12 %. The specific heat capacity of 30 nm nanomaterial was enhanced by an average of 19 %. The specific heat capacity of 60 nm nanomaterial was enhanced by an average of 27 % than the pure eutectic. Measurement uncertainty was found to be less than 3 %. To verify the measurement accuracy, the specific heat capacity of the pure eutectic was compared with the literature value ( 1.50-1.53 kJ/kgC) and made a good agreement. [33] The error was less than 5%. Fig. 3.1 shows cp vs. temperature of pure sample relative to 5nm, 10nm, 30nm, and 60nm nanomaterial tested.

Table 3.1. Specific heat capacity of base eutectic and nanomaterials (solid phase)

cp (kJ/kgC)	Base eutectic	nanomaterial (5nm)	nanomaterial (10nm)	nanomaterial (30nm)	nanomaterial (60nm)
1st sample	1.24	1.28	1.29	1.34	1.31
2nd sample	1.20	1.31	1.24	1.25	1.31
3rd sample	1.23	1.21	1.26	1.24	1.36
4th sample	1.20	1.22	1.2	1.25	1.31
5th sample	1.20	1.24	1.29	1.28	1.41
Average	1.21	1.25	1.26	1.27	1.34
Enhancement	-	3%	3%	5%	10%
Standard deviation	0.02	0.04	0.04	0.04	0.04

Table 3.2. Specific heat capacity of base eutectic and nanomaterials (liquid phase)

cp (kJ/kgC)	Base eutectic	nanomaterial (5nm)	nanomaterial (10nm)	nanomaterial (30nm)	nanomaterial (60nm)
1st sample	1.5	1.62	1.69	1.72	1.76
2nd sample	1.45	1.62	1.57	1.71	1.77
3rd sample	1.48	1.59	1.63	1.71	1.82
4th sample	1.44	1.56	1.58	1.72	1.77
5th sample	1.46	1.57	1.65	1.76	1.90
Average	1.47	1.59	1.62	1.72	1.80
Enhancement	-	10%	13%	21%	28%
Standard deviation	0.02	0.03	0.05	0.02	0.06



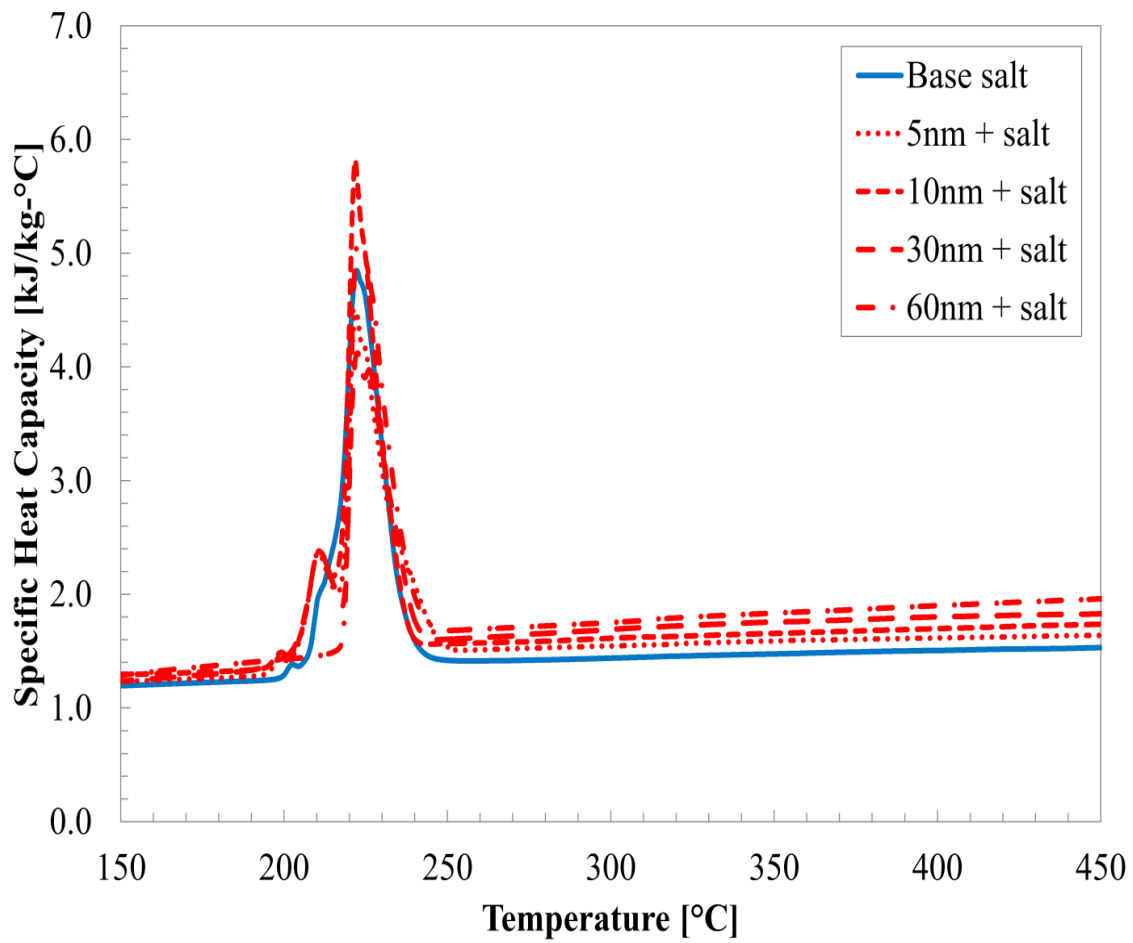


Figure 3.1. The variation of specific heat capacity with temperature for the pure eutectic and the nanomaterials (5 nm, 10 nm, 30 nm and 60 nm) in the full temperature range (150 C – 450 C)..

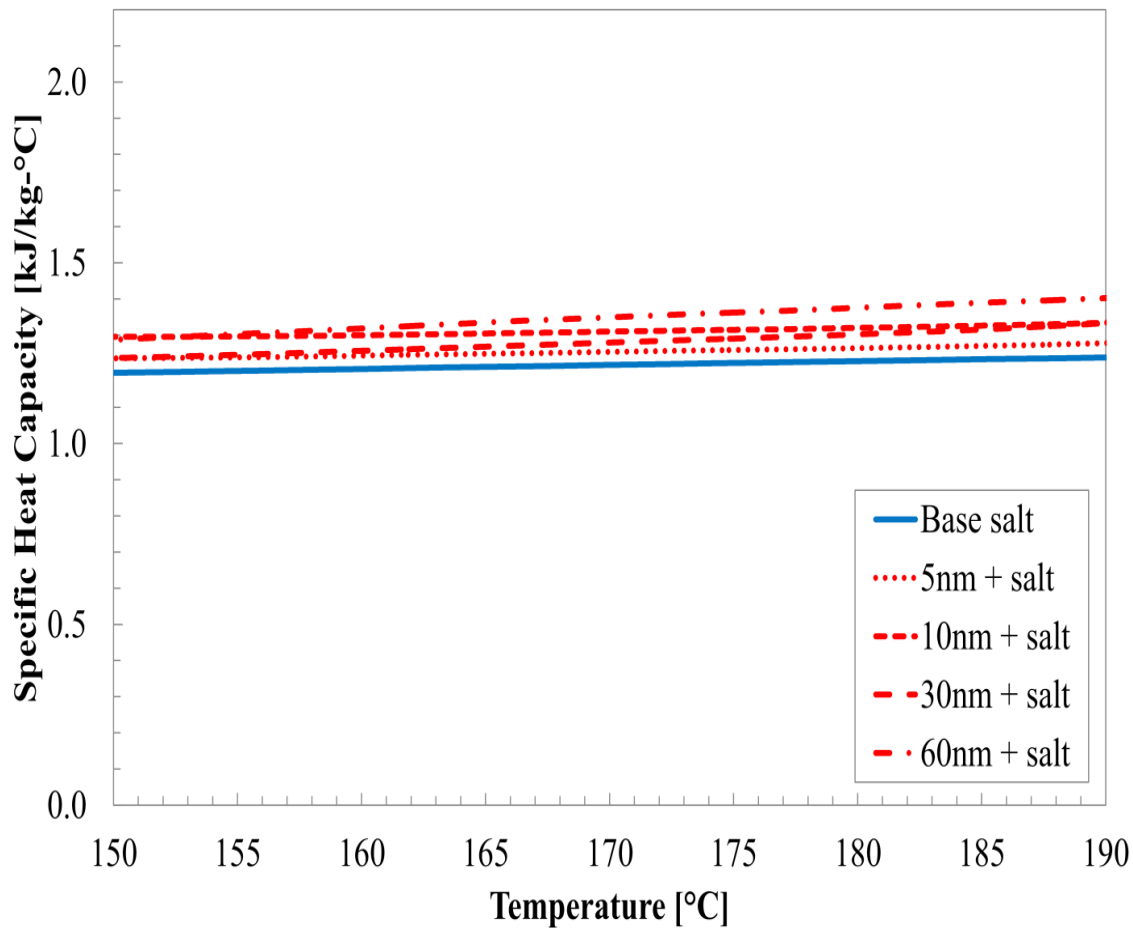


Figure 3.2. The variation of specific heat capacity with temperature for the pure eutectic and the nanomaterials (5 nm, 10 nm, 30 nm and 60 nm) in the solid phase (150 C – 190 C). The specific heat capacity of nanomaterials samples were enhanced by 3-10 % in comparison with the pure eutectic and slightly increased with nanoparticle size..

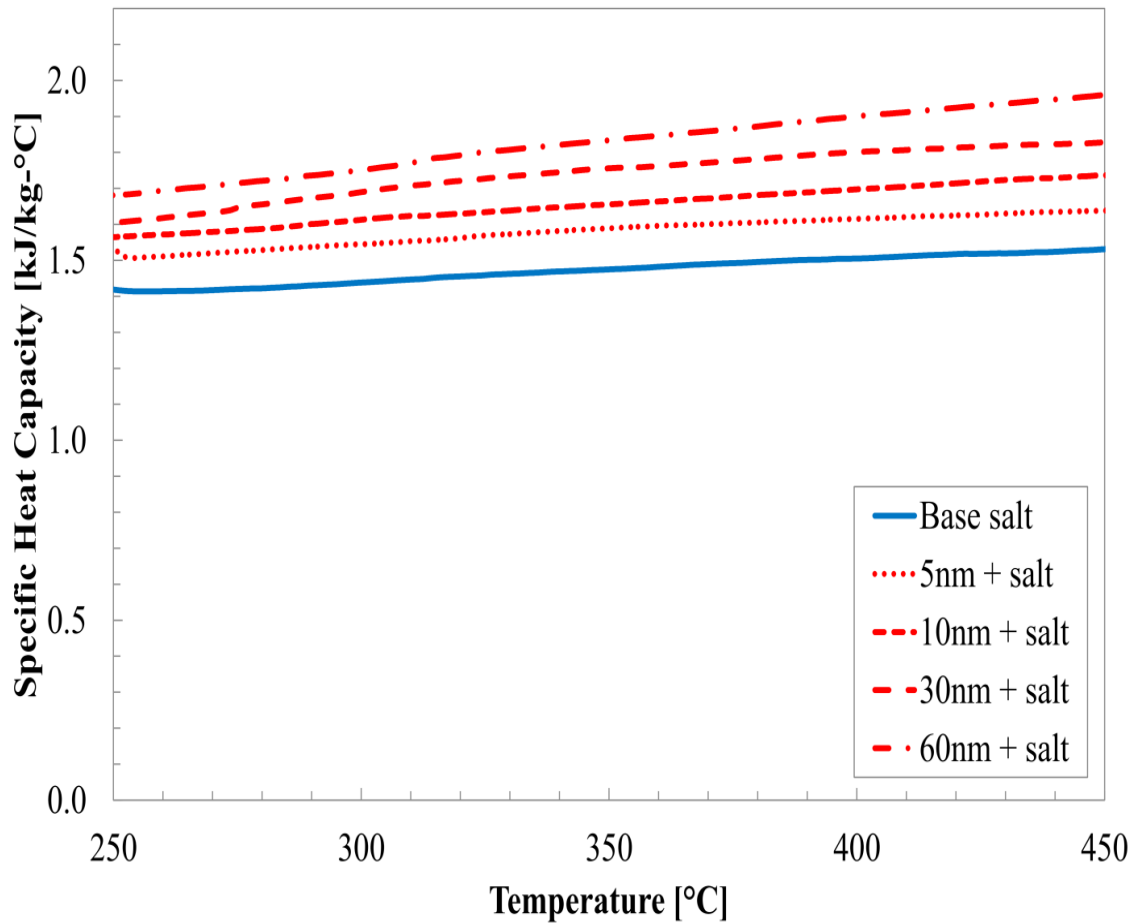


Figure 3.3. The variation of specific heat capacity with temperature for the pure eutectic and the nanomaterials (5 nm, 10 nm, 30 nm and 60 nm) in the liquid phase (250 C – 450 C). The specific heat capacity of nanomaterials samples were enhanced by 10-28 % in comparison with the pure eutectic and increased with nanoparticle size..

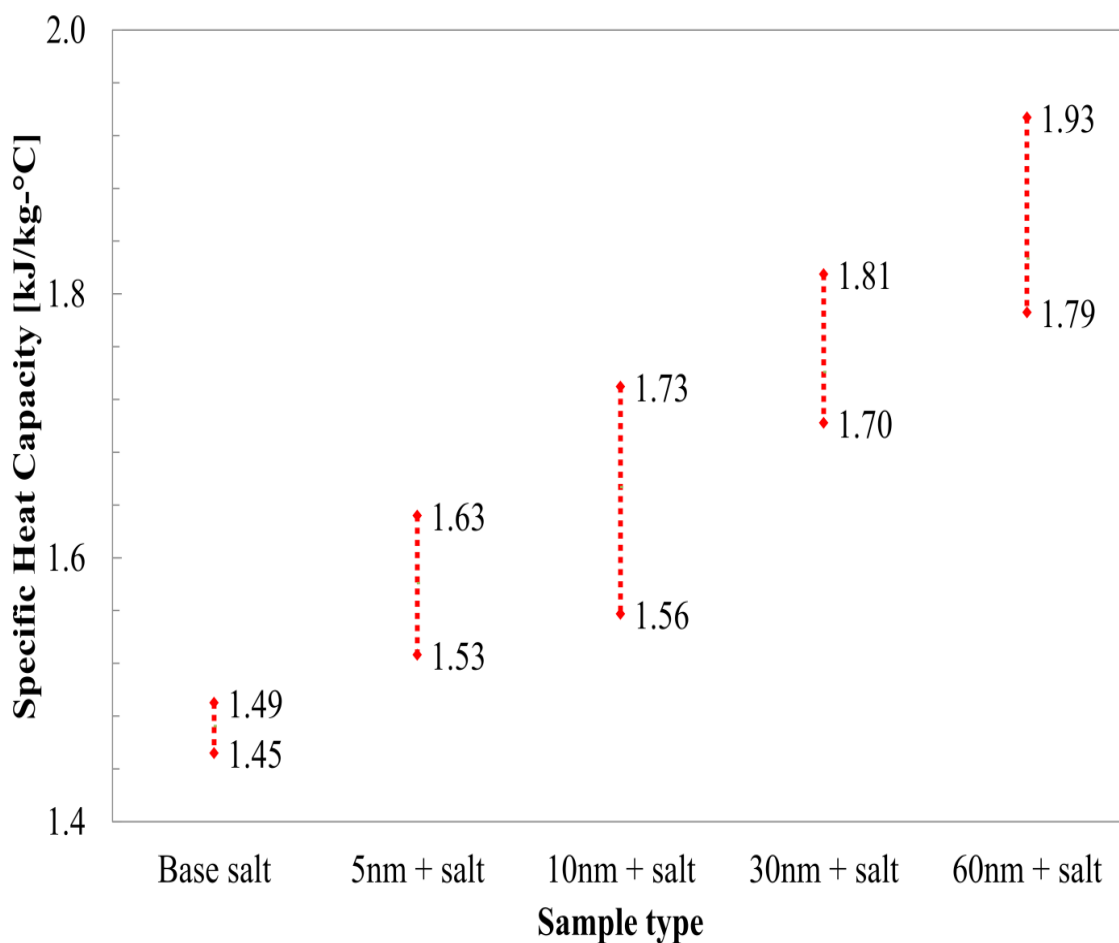


Figure 3.4. The variation of specific heat capacity with different nanoparticle sizes (liquid phase)..

### 3.2 Material characterization

Generally, the enhancement of the specific heat capacity is dependent on the phase or structure of the material. Thus it was necessary to conduct a material characterization to study the structural changes. The changes in structure of the nanomaterials with enhancement compared to the pure sample were stored and analyzed. When the nanomaterials were put to test under the microscope it was observed that there were strange structures at microscale at most parts of the sample. The area

where these special structures were found was focused at high resolution in secondary lens as shown in the figure 4.10. Within this area, salt eutectic molecules seem to form very small structures resembling particles, threads, or webs at the size of 10-100 nm. These special structures when studied in the BSD lens clearly showed a different contrast than the two materials present in the eutectic. This clearly showed that the special structures were additional structures present only in the nanomaterials. It was also evident that they were caused by the addition of nanoparticles. The difference in contrast of those structures are clearly shown in the figures (14-20) below. All the SEM images have been captured at the same resolution and focus so as to get a good comparison between the sizes. According to the literature, salt eutectics are likely to form nanostructures (resembling thread or web patterns) near nanoparticles.[35] These nanostructures are expected to have very high specific surface area compared to the bulk material. Thus this excess surface area might give the edge for the material to hold more heat per unit area thus enhancing the specific heat capacity.[35]

When nanomaterials of all the sizes tested were put under study, it was noticed that the nanostructures were present in all the nanomaterials tested. But these nanostructures were hard to find in 5nm or 10nm samples which had relatively less enhancement. But the nanostructures were more easily visible and were present in huge quantities compared to the 5nm and 10nm in the 30nm and 60nm(Since 30nm and 60nm had higher enhancement than 5nm and 10nm nanomaterial). The maximum number of nanostructures were present in the 60nm sample which was the highest enhanced sample of the lot. It was evident that more nanostructures were present in the nanomaterials with higher sized nanoparticles.It was analyzed that the nanomaterials with higher number of nanostructures had higher enhancement however the reason behind the formation of these nanostructures only in higher sized nanoparticles were still unclear. Thus it was deduced that the presence of nanostructures can increase

the specific heat capacity and not the size of the nanoparticle. The figure 1 3.5 shows the structure of the pure eutectic (in BSD image) which has no strange structures or any special structure. But when we move to the 3.6 we can find some irregularities in the structure of the salt. When clearly observed at high resolution it was noticed that there were presence of nanostructures at all the parts of the sample as shown in figure 3.10. These nanostructures seem to increase and become slightly more visible in 10nm as shown in the figure 3.7. There were clear increase in the amount of nanostructures as we move from 5nm to 10nm to 30nm and 60nm. The nanostructures in the 30nm and 60nm are shown in the figure 3.8 and 3.9 respectively. All the figures below are taken in the BSD lens to distinguish the difference between the nanostructures and the phase structure of the material.

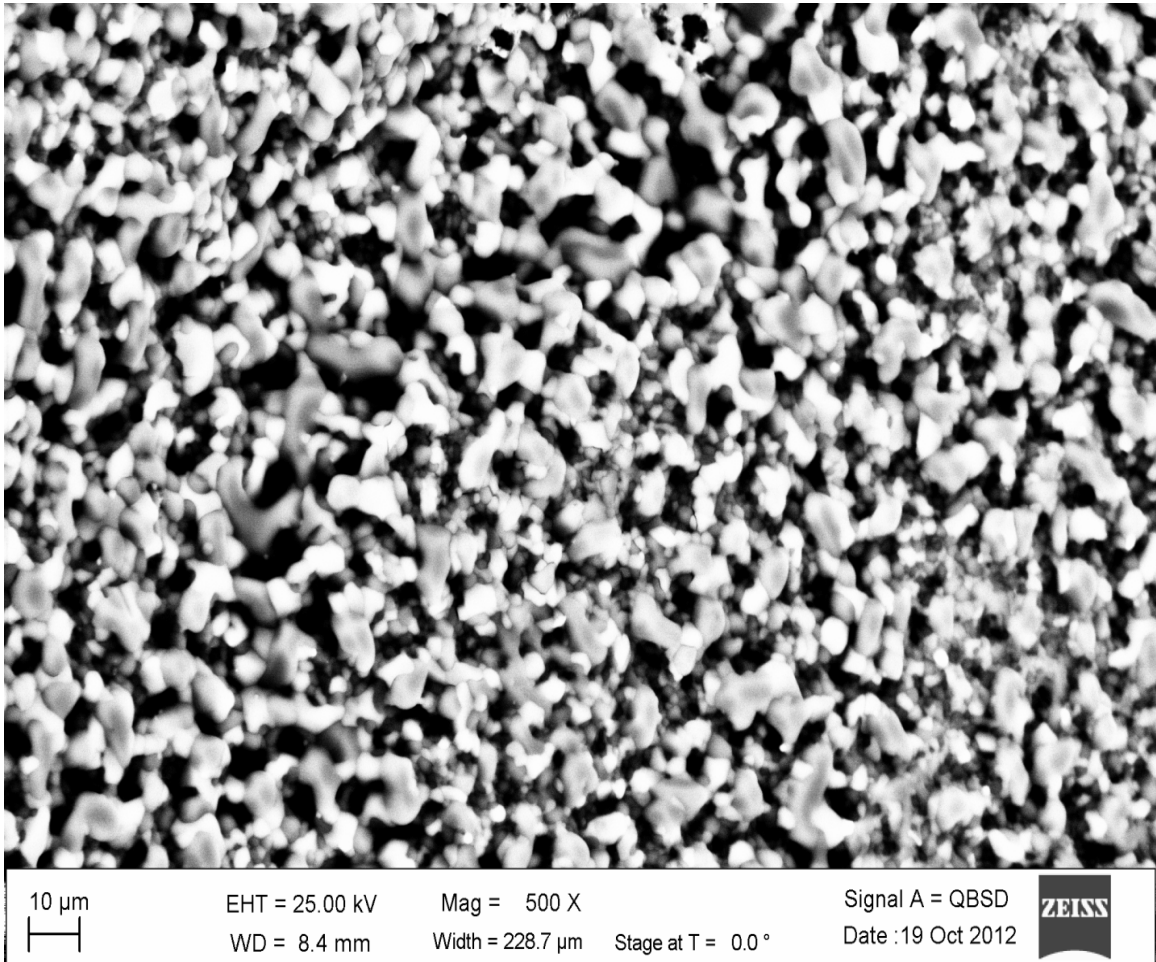


Figure 3.5. The pure nitrate eutectic structure without nanoparticles. This is a back scattered electron image and no significant difference in contrast was observed..

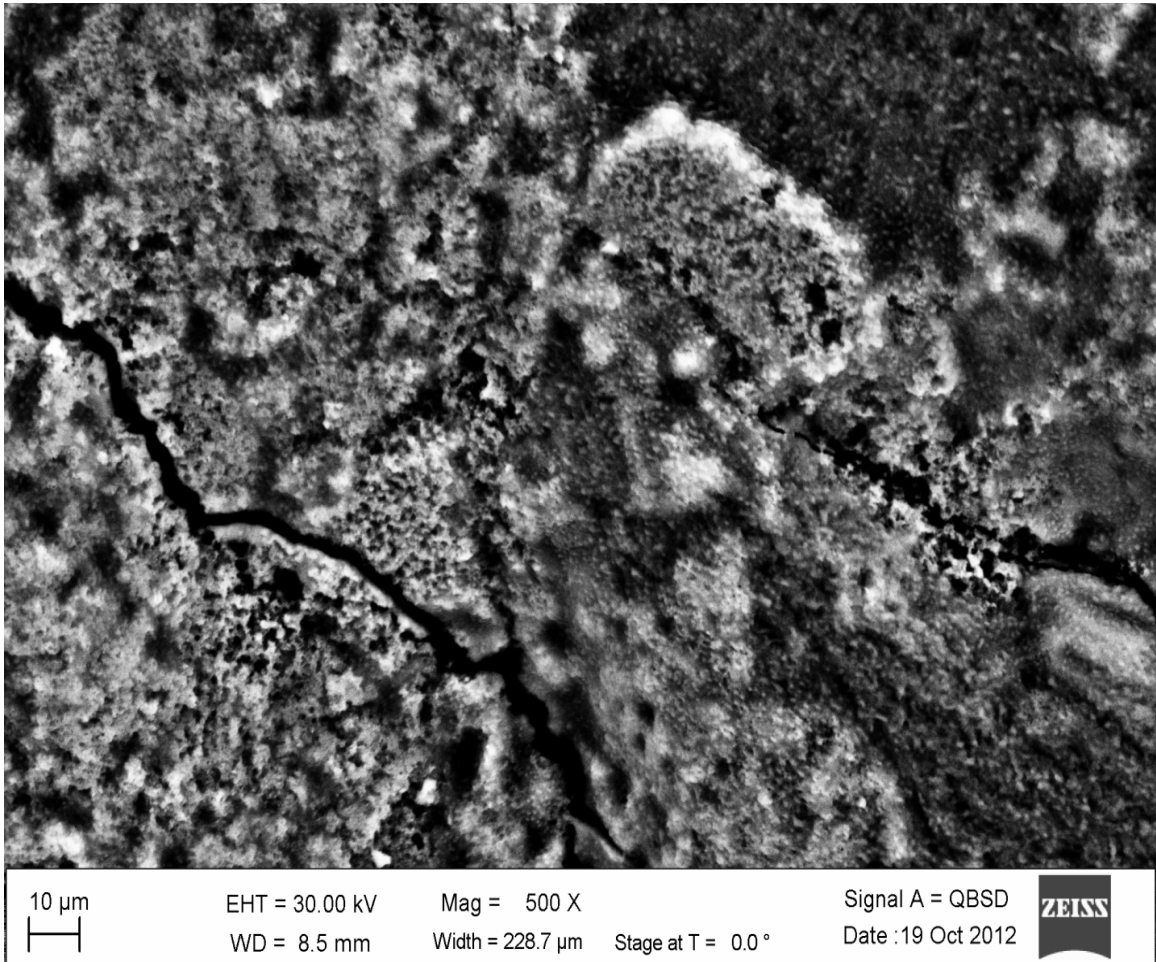


Figure 3.6. 5 nm nanomaterial structure. Comparing with pure eutectic structure (Fig. 3.5), a few small structural changes are rarely observed. (bright area in the image) A high resolution image of these changes is available in Fig. 3.10. This sample shows less than 10 % enhanced specific heat capacity compared with that of pure salt eutectic..



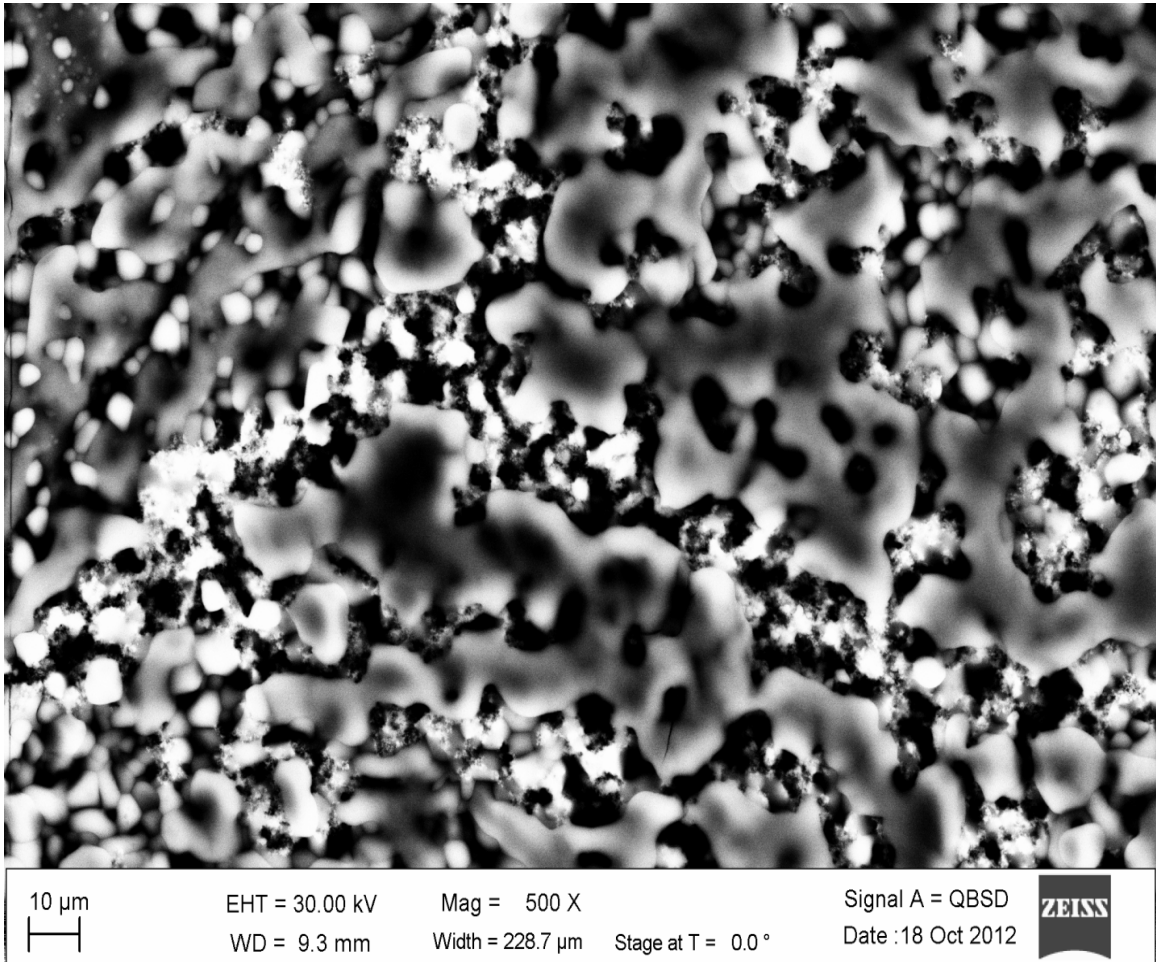


Figure 3.7. 10 nm nanomaterial structure. The contrast difference shown in the backscattered electron image clearly shows the nanostructures formed by the salt eutectic. Comparing with 5 nm nanomaterial (Fig. 3.6), the observed amount of nanostructures is increased. This sample shows 13 % enhanced specific heat capacity compared with that of pure salt eutectic..

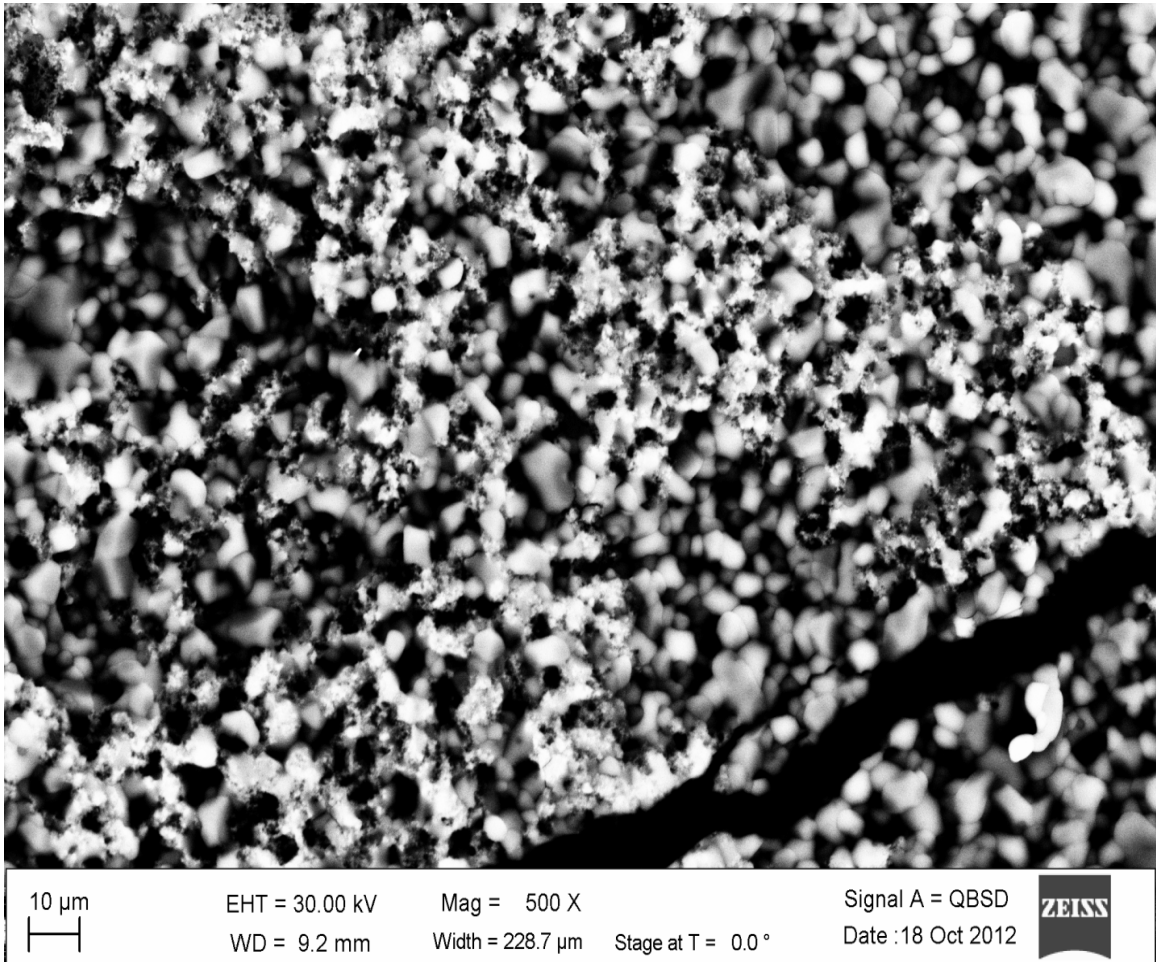


Figure 3.8. 30 nm nanomaterial structure. The contrast difference shown in the backscattered electron image clearly shows the nanostructures formed by the salt eutectic. The quantitative increase of nanostructures is clearly visible here. The amount of nanostructures clearly increased compared with 5 nm (Fig. 3.6) and 10 nm (Fig. 3.7) samples. This sample shows 21 % enhanced specific heat capacity compared with that of pure salt eutectic..

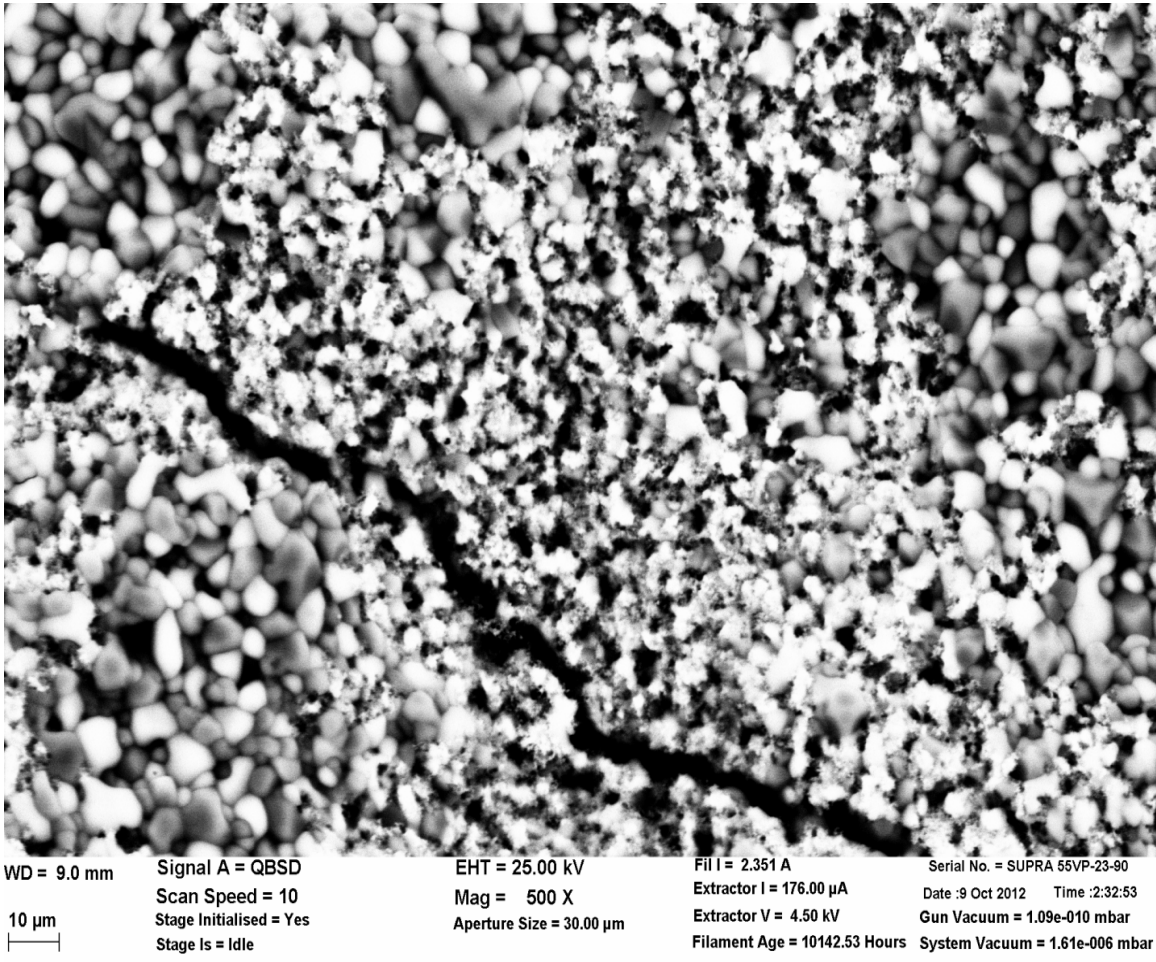


Figure 3.9. 60 nm nanomaterial structure. This sample shows the highest enhancement in specific heat capacity (28 %) compared with that of pure salt eutectic. It is shown in the figure that nanostructures are present almost everywhere. The presence of the large amount of nanostructures can be responsible for the high enhancement in specific heat capacity..

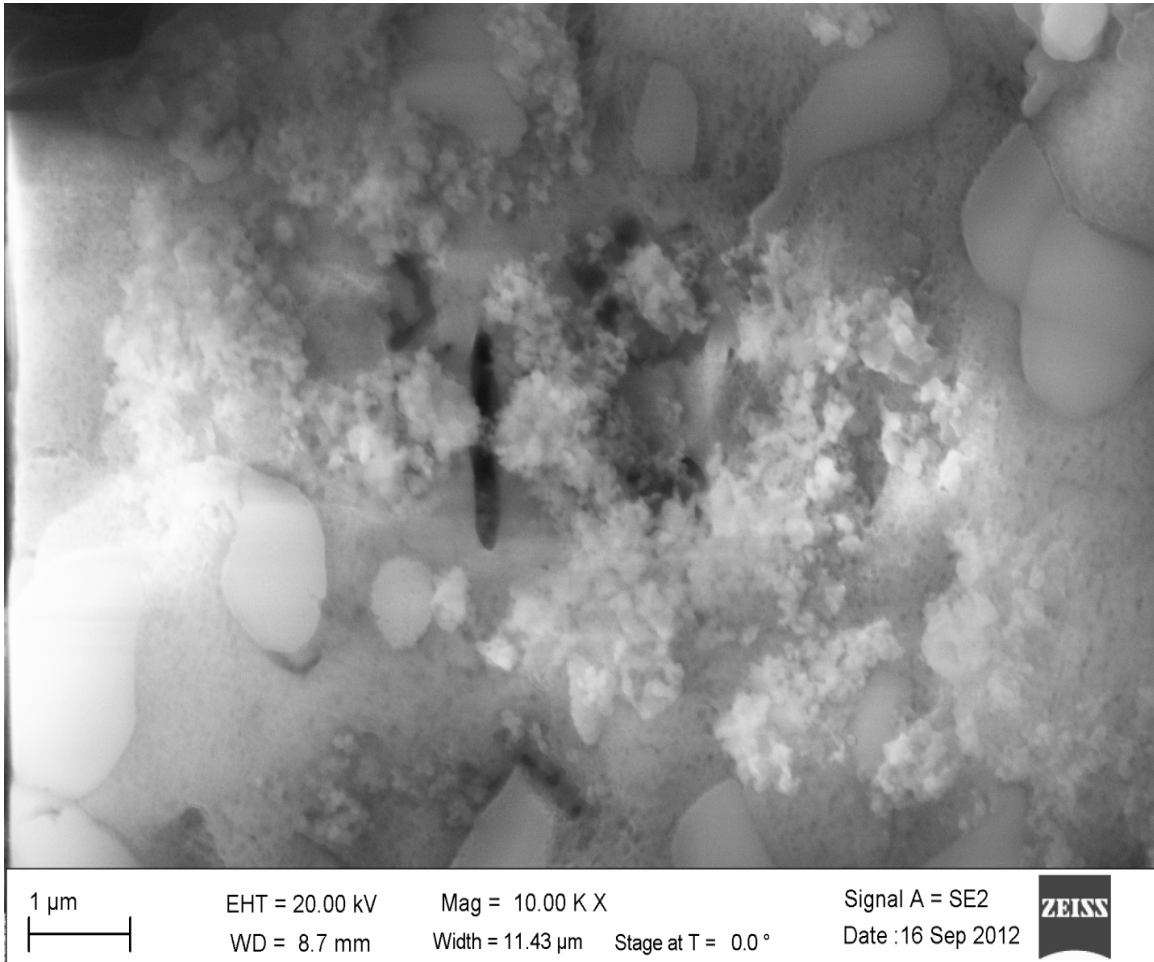


Figure 3.10. A high resolution image of the small structural change found in 5 nm nanomaterial (Fig. 3.6). In this portion of nanomaterial, salt eutectic molecules seem to form very small structures resembling particles, threads, or webs at the size of 10-100 nm (nanostructure)..

### 3.3 Nanostructures

Earlier, Shin and Banerjee [41] had proposed the presence of nanostructures enhancing the specific heat capacity in their study about the molten chloride salts doped with the nanoparticles. Surprisingly, the results obtained in this research makes a good agreement with that results and study. Since the gradual increase of specific heat capacity of nanomaterials with increase in amount of nanostructures

were observed, these nanostructures were deduced to be the reason behind the enhancement. Since nanoparticles have a very large surface area per unit volume, It leads to a large increase in exterior atoms relative to the interior atoms compared to bulk material. Thus the role of surface phonons on specific heat capacity becomes a vital factor for the heat capacity mechanism of nanoparticles and thus nanoparticles have higher specific heat capacity than the bulk. Wang et al [43] theoretically proved the surface effect on the specific heat capacity on the nanoparticle. Wang et al [44] also experimentally proved an enhancement of specific heat capacity of  $Al_2O_3$  nanoparticles by 25%. Similarly, the nanostructures shown in the material characterization also have very large specific surface area. Hence, the specific heat capacity of nanostructure can be also significantly enhanced as nanoparticles and contributes to the enhanced specific heat capacity of nanomaterial.

There should be a localized chemistry change within the salt mixture. When oxide nanoparticles are doped in the salt mixture, hydroxide ( $OH^-$ ) layer is formed on the surface of the nanoparticle. Since the layer formed on the surface is of the negative charge all the positively charged ion in the salt mixture ( $Na^+, K^+$  in this case) will react with the  $OH^-$  layer on the nanoparticles. This is expected to happen as the salt mixture used here is an eutectic of two salts with different melting points. Hence there would be a possibility of molten state with solid and thus there must be a temperature gradient. This interaction leads each salt mixture to move away separately and get crystallized which is deduced to be the origin of nanostructure. However, it is unclear why the amount of nanostructure formations increases with nanoparticle size and it is also evident that the nanostructures are directly influenced by the nanoparticle size. But the heat capacity enhancement is dependent on the increased surface area of nanostructures but independent of nanoparticle size. The reasons behind the formation of nanostructures and its dependence on the size of

nanoparticle are still unknown. (Subject of ongoing research) Possible explanation include: 1) the dispersion ability of nanoparticles relies on the size of nanoparticles. It is possible that too small nanoparticles (5 nm and 10 nm) may not be properly dispersed but precipitated and this hinders the formation of nanostructures. 2) It is possible that too small nanoparticles are likely to agglomerate and may minimize the formation of nanostructures. (This is the subject of on-going research in our group).

Generally, the enhancement of the specific heat capacity is dependent on the phase or structure of the material. Thus it was evident that there must be a change in structure of the material if there is a certain enhancement each time the nanoparticles were doped. Moreover, The change in enhancement when the size was varied made it much convincing that a study must be carried out to observe the changes at microscale in nanomaterials with huge enhancement. Thus the next part of the experiment was to carry out the material characterization.

## CHAPTER 4

### CONCLUSION

In this study, we investigated the specific heat capacity of silica nanoparticle doped Hitec solar salt  $\text{NaNO}_3\text{-KNO}_3$  eutectic (60:40 by weight) . Four different sizes of nanoparticles were doped varying from 5nm to 60nm ( $\text{SiO}_2$  nanoparticles 1% by weight) to test the molten salt nanomaterials for HTF/TES applications in CSP. The specific heat capacity was noted down from the graph of the Modulated differential scanning calorimeter (MDSC) as function of temperature. The specific heat capacity was measured at both solid and liquid phase. The average enhancement of specific heat capacity of the nanomaterials doped with 5nm, 10nm, 30nm and 60nm were found to be 3-10% in the solid phase and 8-28% in the liquid phase respectively. Material characterization was carried out to study the structural changes once the nanoparticles are doped. It was found that special nanostructures were formed in the salt mixture. The possible explanations behind the formation of such structures were discussed and the same was deduced to be the cause for the anomalous enhancement of specific heat capacity. It was observed as the amount of nanostructures increased with each nanomaterial. It was deduced that the amount of nanostructures impacts the specific heat capacity of the nanomaterial. Hence more the nanostructures more would be the specific heat capacity. According to the literature [41] nanostructures have a very large specific surface area and this significantly amplifies the contribution of surface energy on the specific heat capacity.

Using these nanomaterials with improved specific heat capacity as HTF in CSP systems can significantly reduce the necessary amount of HTF material, the size of

thermal transport system, thermal storage system, and thus will help to reduce the cost of electricity produced by CSP.



## REFERENCES

- [1] “Block diagram of csp.” [Online]. Available: <http://www.volker-quaschning.de/articles/fundamentals2/index.php>
- [2] P. E. Glaser, “Power from the Sun: its future,” *Science*, vol. 162, pp. 857–861, 1968.
- [3] F. Cavallaro, “Fuzzy topsis approach for assessing thermal-energy storage in concentrated solar power (csp) systems,” *Applied Energy*, vol. 87, no. 2, pp. 496–503, February 2010.
- [4] V. Quaschning and M. Blanco, “Solar power-photovoltaics or solar thermal power?” *Proceedings of VGB Congress Power Plants 2001*, Oct 10-12 2001.
- [5] B. Chiaro, S. Payne, T. Dutzik, and E. A. R. . P. Center, *On the Rise: Solar Thermal Power and the Fight Against Global Warming*. Environment America Research & Policy Center, 2008. [Online]. Available: [http://books.google.com/books?id=\\_7vbtgAACAAJ](http://books.google.com/books?id=_7vbtgAACAAJ)
- [6] B. C. Staley, J. Goodward, C. Rigdon, and A. MacBride, “Juice From Concentrate: Reducing Emissions with Concentrating Solar Thermal Power,” *world resources institute*, May 2009.
- [7] “Picture of a parabolic trough.” [Online]. Available: [http://www.volker-quaschning.de/fotos/psa/Solarchemie\\_1024x768.jpg](http://www.volker-quaschning.de/fotos/psa/Solarchemie_1024x768.jpg)
- [8] “Block diagram of a parabolic trough.” [Online]. Available: <http://ars.els-cdn.com/content/image/1s2.0S1364032109001294gr1.jpg>

- [9] U. D. of Energy, “Dish/engine systems for concentrating solar power,” feb 2013. [Online]. Available: [http://www.eere.energy.gov/basics/renewable\\_energy/dish\\_engine.html](http://www.eere.energy.gov/basics/renewable_energy/dish_engine.html)
- [10] “Picture of a concentrating dish.” [Online]. Available: [http://yes2renewables.files.wordpress.com/2012/03/solar\\_systems\\_dish%20-91.jpg](http://yes2renewables.files.wordpress.com/2012/03/solar_systems_dish%20-91.jpg)
- [11] “Block diagram of a concentrating dish.” [Online]. Available: [http://3.bp.blogspot.com/\\_b5hcKABPIGI/SmT3PeHvXoI/AAAAAAAAAXHo/Bkt5-RvQPhI/s400/5-2509a.jpg](http://3.bp.blogspot.com/_b5hcKABPIGI/SmT3PeHvXoI/AAAAAAAAAXHo/Bkt5-RvQPhI/s400/5-2509a.jpg)
- [12] M. Mesanovic and N. Philippsen, “Solar Power Towers,” dec 1996. [Online]. Available: [http://lisas.de/projects/alt\\_energy/sol\\_thermal/powertower.html](http://lisas.de/projects/alt_energy/sol_thermal/powertower.html)
- [13] “Picture of a power tower.” [Online]. Available: [http://www.abengoa.com/export/sites/abengoa\\_corp/resources/gestion\\_noticias/images/es/Three](http://www.abengoa.com/export/sites/abengoa_corp/resources/gestion_noticias/images/es/Three)
- [14] “Block diagram of a power tower.” [Online]. Available: <http://webservices.itcs.umich.edu/drupal/recd/sites/webservices.itcs.umich.edu.drupal.recd/files/2.jpg>
- [15] t. . P. National Renewable Energy Laboratory, jan 2010. [Online]. Available: [http://www.nrel.gov/csp/troughnet/thermal\\_energy\\_storage.html](http://www.nrel.gov/csp/troughnet/thermal_energy_storage.html)
- [16] B. Kelly and D. Kearney, “Thermal storage commercial plant design study for a 2-tank indirect molten salt system,” 2006.
- [17] R. E. Project, “Andasol-1 thermo solar energy .” [Online]. Available: <http://www.estelasolar.eu/fileadmin/ESTELAdocs/documents/powerplants/Andasol.pdf>
- [18] M. J. Kelly, P. F. Hlava, and D. A. Brosseau, “Testing thermocline filler materials and molten-salt heat transfer fluids for thermal energy storage systems used in parabolic trough solar power plants.” Sandia National Laboratories, Tech. Rep., 2004.

- [19] U. Herrmann, B. Kelly, and H. Price, “Two-tank molten salt storage for parabolic trough solar power plants,” *Energy*, vol. 29, pp. 883 – 893, 2004. [Online]. Available: <http://www.sciencedirect.com/science/article/pii/S0360544203001932>
- [20] P. H. Muller, “Solar Thermal power plants: On the way to commercial market introduction.” [Online]. Available: <http://www.htri.net/Public/prodsvcs/HMS-Victoria1.pdf>
- [21] D. Kearney, U. Herrmann, P. Nava, B. Kelly, R. Mahoney, J. Pacheco, R. Cable, N. Potrovitza, D. Blake, and H. Price, “Assessment of a molten salt heat transfer fluid in a parabolic trough solar field,” *TRANSACTIONS-AMERICAN SOCIETY OF MECHANICAL ENGINEERS JOURNAL OF SOLAR ENERGY ENGINEERING*, vol. 125, no. 2, pp. 170–176, 2003.
- [22] S. W. Paper, “Molten salt as heat transfer fluid ,” 2011. [Online]. Available: <http://www.skyfuel.com/downloads/brochure/MoltenSaltasHeatTransferFluid.pdf>
- [23] G. Janz and R. P. I. M. S. D. Center, *Physical properties data compilations relevant to energy storage...: data on additional single and multi-component salt systems. Molten salts*, ser. NSRDS-NBS. U.S. Dept. of Commerce, National Bureau of Standards : for sale by the Supt. of Docs., U.S. Govt. Print. Off., 1981.
- [24] S. Millenium, “The parabolic trough power plants from Andasol 1-3,” 2008. [Online]. Available: <http://www.rwe.com/web/cms/mediablob/en/1115150/data/1115144/1/rwe-innogy/sites/solar-power/andasol-3/facts-figures/Further-information-about-Andasol.pdf>
- [25] R. energy world, “storing the sun: Molten salt provides highly efficient thermal storage.” [Online]. Available:

<http://www.renewableenergyworld.com/rea/news/article/2008/06/storing-the-sun-molten-salt-provides-highly-efficient-thermal-storage-52873>

- [26] R. Bradshaw and D. Meeker, “High-temperature stability of ternary nitrate molten salts for solar thermal energy systems,” *Solar energy materials*, vol. 21, no. 1, pp. 51–60, 1990.
- [27] R. kb, “Molten nitrate salt for solar energy storage,” october 11 2009. [Online]. Available: <http://www.energystoragenews.com/Molten%20Nitrate%20Salt%20for%20Solar%20Energy%20St>
- [28] N. Araki, M. Matsuura, A. Makino, T. Hirata, and Y. Kato, “Measurement of thermophysical properties of molten salts: Mixtures of alkaline carbonate salts,” *International Journal of Thermophysics*, vol. 9, no. 6, pp. 1071–1080, 1988.
- [29] H. Price, E. Lüpfert, D. Kearney, E. Zarza, G. Cohen, R. Gee, and R. Mahoney, “Advances in parabolic trough solar power technology,” *Journal of solar energy engineering*, vol. 124, no. 2, pp. 109–125, 2002.
- [30] N. J. Bridges, A. E. Visser, and E. B. Fox, “Potential of nanoparticle-enhanced ionic liquids (neils) as advanced heat-transfer fluids,” *Energy and Fuels*, vol. 25, no. 10, p. 4862, 2011.
- [31] S. U. Choi and J. Eastman, “Enhancing thermal conductivity of fluids with nanoparticles,” Argonne National Lab., IL (United States), Tech. Rep., 1995.
- [32] J. Eastman, U. Choi, S. Li, L. Thompson, and S. Lee, “Enhanced thermal conductivity through the development of nanofluids,” in *Materials Research Society Symposium Proceedings*, vol. 457. Cambridge Univ Press, 1997, pp. 3–12.
- [33] S. Shaikh, K. Lafdi, and R. Ponnappan, “Thermal conductivity improvement in carbon nanoparticle doped pao oil: An experimental study,” *Journal of Applied Physics*, vol. 101, no. 6, pp. 064 302–064 302, 2007.

- [34] J. Eastman, S. Choi, S. Li, W. Yu, and L. Thompson, “Anomalously increased effective thermal conductivities of ethylene glycol-based nanofluids containing copper nanoparticles,” *Applied Physics Letters*, vol. 78, no. 6, pp. 718–720, 2001.
- [35] S. Lee, U. Choi, STEPHEN, S. Li, and J. Eastman, “Measuring thermal conductivity of fluids containing oxide nanoparticles,” *Journal of Heat Transfer*, vol. 121, no. 2, 1999.
- [36] S. Choi, Z. Zhang, W. Yu, F. Lockwood, and E. Grulke, “Anomalous thermal conductivity enhancement in nanotube suspensions,” *Applied Physics Letters*, vol. 79, no. 14, pp. 2252–2254, 2001.
- [37] S. P. Jang and S. U. Choi, “Role of brownian motion in the enhanced thermal conductivity of nanofluids,” *Applied physics letters*, vol. 84, no. 21, pp. 4316–4318, 2004.
- [38] P. Keblinski, S. Phillpot, S. Choi, and J. Eastman, “Mechanisms of heat flow in suspensions of nano-sized particles (nanofluids),” *International journal of heat and mass transfer*, vol. 45, no. 4, pp. 855–863, 2002.
- [39] I. C. Nelson, D. Banerjee, and R. Ponnappan, “Flow loop experiments using polyalphaolefin nanofluids,” *Journal of Thermophysics and Heat Transfer*, vol. 23, no. 4, pp. 752–761, 2009.
- [40] S.-Q. Zhou and R. Ni, “Measurement of the specific heat capacity of water-based  $\text{Al}_2\text{O}_3$  nanofluid,” *Applied Physics Letters*, vol. 92, no. 9, pp. 093 123–093 123, 2008.
- [41] D. Shin and D. Banerjee, “Enhancement of specific heat capacity of high-temperature silica-nanofluids synthesized in alkali chloride salt eutectics for solar thermal-energy storage applications,” *International journal of heat and mass transfer*, vol. 54, no. 5, pp. 1064–1070, 2011.

- [42] M. Betts, “The effects of nanoparticle augmentation of nitrate thermal storage materials for use in concentrating solar power applications,” 2013.
- [43] B.-X. Wang, L.-P. Zhou, and X.-F. Peng, “Surface and size effects on the specific heat capacity of nanoparticles,” *International journal of thermophysics*, vol. 27, no. 1, pp. 139–151, 2006.
- [44] L. Wang, Z. Tan, S. Meng, D. Liang, and G. Li, “Enhancement of molar heat capacity of nanostructured  $\text{Al}_2\text{O}_3$ ,” *Journal of Nanoparticle Research*, vol. 3, no. 5-6, pp. 483–487, 2001.

## BIOGRAPHICAL STATEMENT

Bharath Dudda was born in Shimoga, Karnataka, India in 1988. He received his B.S. degree from Visveshwaraiah Technological University, Belgaum, in 2010, his M.S. degree from The University of Texas at Arlington in 2013, in Mechanical Engineering. He is the eldest child of Father D.C.Srivatsa (Chief manager Indian Overseas Bank) and Mother Roopakala (Housewife). Bharath's younger brother, D.S.Jayanth is persuing his career as an intern in Chartered Accountant. Bharath's field of interest includes the Concentrated Solar power applications. He deals more specifically in the field of thermal energy storage for the concentrated solar power using the nanomaterials. He has two years of experience in nanofabrication and thermal characterization.